

Injured astrocytes are repaired by Synaptotagmin XI-regulated lysosome exocytosis

SC Sreetama¹, T Takano², M Nedergaard², SM Simon³ and JK Jaiswal^{*,1,4}

Astrocytes are known to facilitate repair following brain injury; however, little is known about how injured astrocytes repair themselves. Repair of cell membrane injury requires Ca²⁺-triggered vesicle exocytosis. In astrocytes, lysosomes are the main Ca²⁺-regulated exocytic vesicles. Here we show that astrocyte cell membrane injury results in a large and rapid calcium increase. This triggers robust lysosome exocytosis where the fusing lysosomes release all luminal contents and merge fully with the plasma membrane. In contrast to this, receptor stimulation produces a small sustained calcium increase, which is associated with partial release of the lysosomal luminal content, and the lysosome membrane does not merge into the plasma membrane. In most cells, lysosomes express the synaptotagmin (Syt) isoform Syt VII; however, this isoform is not present on astrocyte lysosomes and exogenous expression of Syt VII on lysosome inhibits their exocytosis. Deletion of one of the most abundant Syt isoform in astrocyte – Syt XI – suppresses astrocyte lysosome exocytosis. This identifies lysosome as Syt XI-regulated exocytic vesicle in astrocytes. Further, inhibition of lysosome exocytosis (by Syt XI depletion or Syt VII expression) prevents repair of injured astrocytes. These results identify the lysosomes and Syt XI as the sub-cellular and molecular regulators, respectively of astrocyte cell membrane repair.

Cell Death and Differentiation (2016) 23, 596–607; doi:10.1038/cdd.2015.124; published online 9 October 2015

Astrocyte secretion through membrane channels,¹ exocytosis of small synaptic-like vesicles (SSLV; 30–50 nm)^{2–4} and large vesicles (>200 nm)^{2,5–7} regulate neuronal and vascular functions.^{8–10} Lysosomes are large, and the major Ca²⁺-triggered exocytic vesicles in astrocytes.^{11,12} Whereas receptor signaling triggers lysosome exocytosis in astrocytes, in other cell types, cell membrane damage is a potent trigger of lysosome exocytosis.^{13–16} Lysosome exocytosis facilitates repair of injured cells,¹⁴ and through secretion of adenosine triphosphate (ATP), cytokines and cytolytic proteins also facilitates repair of injured tissue.^{17–19} Although the role of lysosomal exocytosis in ATP secretion by astrocytes has been documented, its role in astrocyte cell membrane repair has not been examined.^{20,21}

Regulated exocytosis involves SNAREs (soluble N-ethylmaleimide-sensitive factor attachment protein receptors) and calcium-sensing protein Syt. SNAREs present on the opposing membranes interact with each other to assemble into a *trans*-SNARE complex.²² Subsequently, calcium binding to the C2 domains of synaptotagmin triggers full *trans*-SNARE assembly, which provides the force needed for vesicle fusion.²³ About half of all Syt isoforms have been shown to be non-Ca²⁺ binding and even the Ca²⁺-binding Syts are known to regulate Ca²⁺-independent steps such as vesicle docking at the target membrane.^{24–26} Although Syt XI is

among the most abundant Syt isoform in astrocytes,²⁷ Syt IV – the only Syt isoform studied in astrocytes – regulates SSLV exocytosis.²⁸ In other cells, lysosome exocytosis is regulated by Syt VII^{15,29} but there is conflicting evidence of Syt VII expression in astrocytes.^{11,20,27,28,30} Thus, the synaptotagmin regulating lysosomal exocytosis in astrocytes is yet to be identified. Further, neuroglial signaling is the only role of Ca²⁺-triggered exocytosis in astrocytes that has been studied.^{8–10}

Using total internal reflection fluorescence (TIRF) microscopy here we have monitored receptor stimulation-triggered and cell membrane injury-triggered exocytosis of individual lysosome in astrocytes and studied its role in cell membrane repair. Injury caused a greater increase in intracellular calcium (cytosolic calcium, [Ca²⁺]_c) than receptor stimulation, which affected the nature and kinetics of lysosome exocytosis. Receptor stimulation caused continued lysosomal fusions where lysosomes partially release their content (partial fusion). In contrast, injury caused a rapid burst of fusion events, and the fusing lysosomes fully released luminal and membrane content (complete fusion). Syt XI, but not Syt VII, was detected on astrocyte lysosomes. Depletion of Syt XI and expression of Syt VII on astrocyte lysosome reduced lysosome exocytosis, prevented full fusion of lysosomes, and compromised the ability of astrocytes to repair. This identifies cell membrane repair as a new role of lysosome exocytosis in

¹Center for Genetic Medicine Research, Children's National Medical Center, 111 Michigan Avenue NW, Washington, DC, USA; ²Center for Translational Neuromedicine, University of Rochester Medical Center, 601 Elmwood Avenue, Rochester, NY, USA; ³Laboratory of Cellular Biophysics, The Rockefeller University, 1230 York Avenue, New York, NY, USA and ⁴Department of Integrative Systems Biology, George Washington University School of Medicine and Health Sciences, 111 Michigan Avenue NW, Washington, DC, USA

*Corresponding author: JK Jaiswal, Department of Integrative Systems Biology, George Washington University School of Medicine and Health Sciences, 111 Michigan Avenue NW, Washington, DC 20010, USA. Tel: +1 202 476 6456; Fax: +1 202 476 6014; E-mail: jkjaishwal@cnmc.org

Abbreviations: ATP, adenosine triphosphate; ASM, acid sphingomyelinase; [Ca²⁺]_c, cytosolic calcium; DHPG, 3,5-Dihydroxyphenylglycine; FITC, fluorescein isothiocyanate; SNARE, soluble N-ethylmaleimide-sensitive factor attachment protein receptors; Syt, synaptotagmin; SytXI^r, siRNA-resistant Syt XI cDNA; SytXI^rDN, siRNA-resistant Syt XI cDNA with aspartate to asparagine mutation; TIRF, total internal reflection fluorescence

Received 22.2.15; revised 03.8.15; accepted 17.8.15; Edited by N Bazan; published online 09.10.15

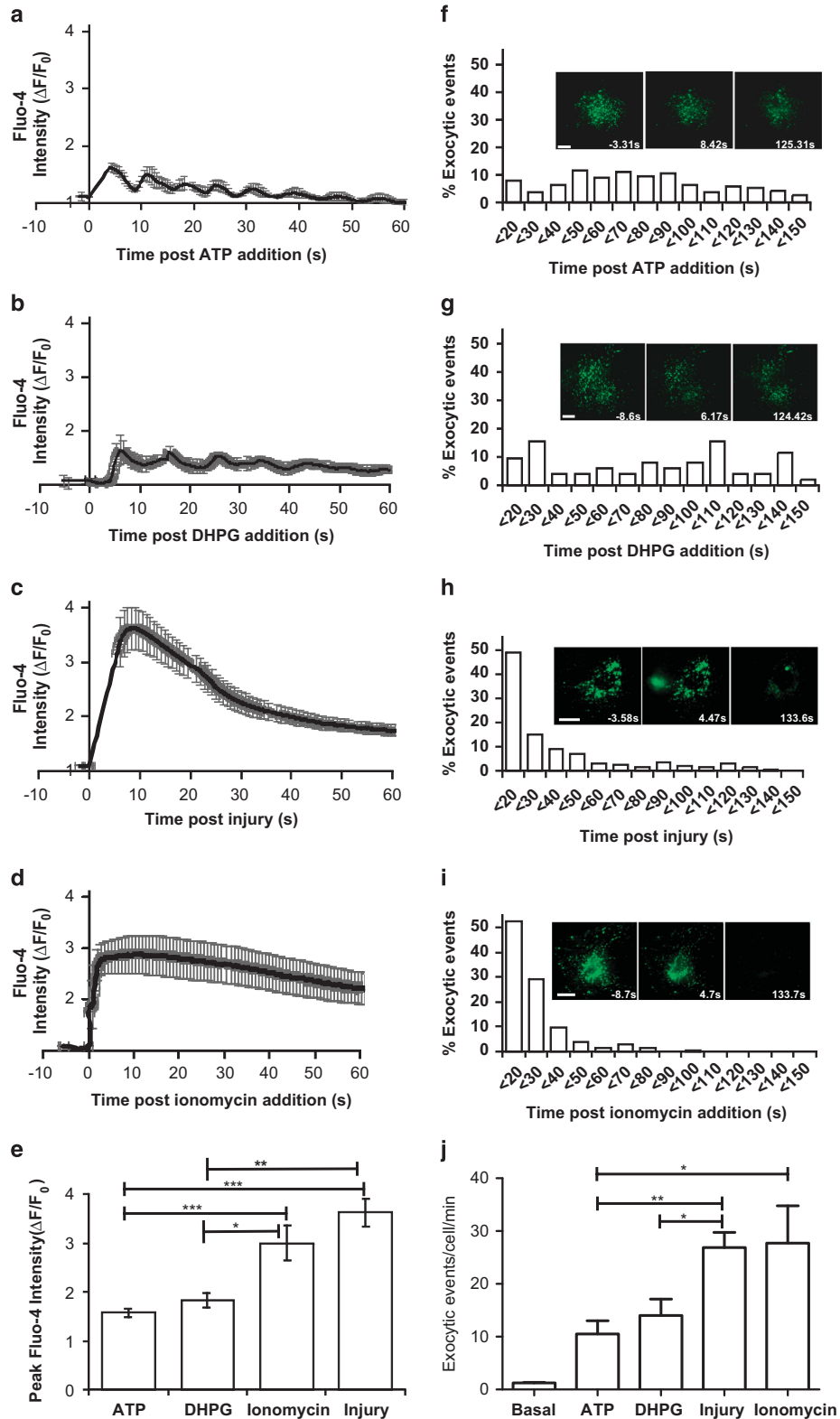


Figure 1 Calcium agonists differentially affect cytosolic calcium and lysosome exocytosis. (a–d) Representative traces of change in cytosolic calcium in primary astrocytes treated with indicated calcium agonist or injured focally by a pulsed laser. (e) Plots showing averaged peak calcium increase measured by Fluo-4 following indicated treatment ($n > 7$ cells each). (f–i) Kinetics of lysosome exocytosis following treatment with (f) 10 μ M ATP ($n = 7$), (g) 10 μ M DHPG ($n = 4$), (h) focal laser injury ($n = 6$) and (i) 10 μ M ionomycin ($n = 10$). Insets show representative frames from TIRF images of lysosomes in a cell treated as indicated in the plot. Scale bars indicate 10 μ m. (j) Plot for number of lysosome exocytic events/cell/min in untreated (basal) or treated by ATP, DHPG, injury and ionomycin. Data represent mean \pm S.E.M.; assessed by Mann–Whitney *U*-test; * $P < 0.05$, ** $P < 0.01$ and *** $P < 0.001$

astrocytes and Syt XI as a regulator of lysosome exocytosis and of astrocyte cell membrane repair.

Results

Differential effect of receptor and injury-triggered Ca^{2+} increase on lysosome exocytosis. To monitor Ca^{2+} -regulated lysosome exocytosis in primary astrocytes, $[\text{Ca}^{2+}]_c$ was raised either indirectly (by activating receptors) or directly (by calcium ionophore or cell membrane injury) – see Materials and Methods. Using calcium indicator Fluo-4, purinergic signaling was observed to cause instantaneous oscillation of $[\text{Ca}^{2+}]_c$ (Figure 1a), whereas metabotropic glutamate receptor signaling caused $[\text{Ca}^{2+}]_c$ to peak with a delay of 5s followed by continued oscillations (Figure 1b). Direct Ca^{2+} entry by focal cell membrane injury by a pulsed laser caused an instantaneous rise in $[\text{Ca}^{2+}]_c$, which decreased over the next minute as the cell repaired (Figure 1c).¹⁶ Calcium ionophore (ionomycin) caused rapid and sustained increase in $[\text{Ca}^{2+}]_c$ (Figure 1d). The amplitude of $[\text{Ca}^{2+}]_c$ increase by injury or ionomycin was twice as large as the receptor-mediated signaling (Figure 1e).

To examine the effect of differential $[\text{Ca}^{2+}]_c$ increase on lysosome exocytosis, individual lysosomes were imaged using TIRF microscopy. Fluorescently labeling lysosomes with fluorescein isothiocyanate (FITC) dextran allows imaging without photodamage.¹² $[\text{Ca}^{2+}]_c$ increase by purinergic signaling triggered sustained FITC dextran-labeled lysosome exocytosis that peaked within a minute, and most fusions occurred within the first 90s of ATP addition (Figure 1f; Supplementary Video 1). Each cell exocytosed 10.5 ± 2.5 lysosomes in a minute (Figure 1j); however, many membrane proximal lysosomes did not exocytose (Figure 1f, inset). Metabotropic signaling also caused sustained lysosomal exocytosis (Figure 1g; Supplementary Video 1), with each cell exocytosing 14.0 ± 3.1 lysosome/minute; again all membrane proximal lysosomes did not exocytose (Figures 1j and g, inset). In contrast to receptor stimulation, direct increase in $[\text{Ca}^{2+}]_c$ by focal cell membrane injury caused the lysosome exocytosis to peak within 10s. Half of all exocytic events occurred by 30s and all fusions ceased by 140s (Figure 1h; Supplementary Video 1). Each cell exocytosed 26.9 ± 2.9 lysosomes/minute, and most of the membrane docked lysosomes underwent exocytosis (Figures 1j and h, inset). Direct $[\text{Ca}^{2+}]_c$ increase by ionomycin caused half of all exocytic

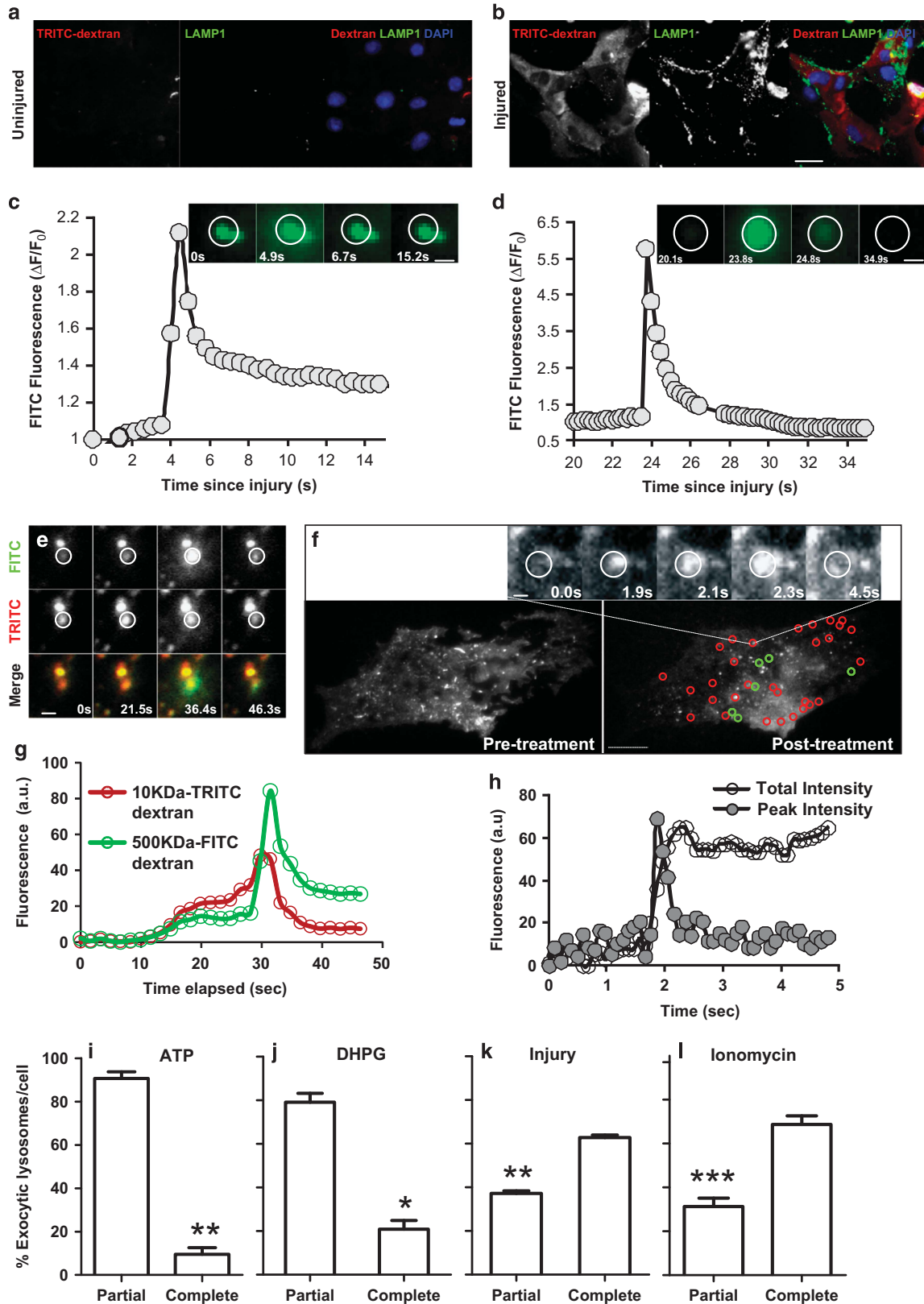
events to occur within the first 20s (Figure 1i; Supplementary Video 1). Each cell exocytosed an average of 27.7 ± 7.1 lysosomes/minute, and all lysosomes at the cell membrane underwent exocytosis within 100s of treatment (Figures 1j and i, inset). Astrocytes derived from mice and rats exhibited similar exocytic response – ionomycin triggered 26.9 ± 2.9 versus 25.2 ± 6.9 exocytic events/minute, respectively. As an alternate assay for injury-triggered lysosomal exocytosis, astrocytes were injured with glass beads (in presence of TRITC dextran to mark injured cells) and cell surface appearance of lysosomal membrane protein (LAMP1) was monitored in live cells using an antibody that binds the luminal domain of LAMP1.³¹ The cell surface LAMP1 level increased in all injured astrocytes, demonstrating injury-triggered lysosome exocytosis (Figures 2a and b).

Lysosome exocytosis in astrocytes is regulated differently compared with that in fibroblasts. Similar to other vesicles,^{32,33} lysosomes can fuse partially, releasing a part of their luminal content, and their membrane does not merge with the plasma membrane.^{29,34} However, the existence of partial exocytosis of astrocyte lysosomes has been contested.^{11,20} Using FITC dextran to label the lysosome lumen, we found that astrocyte lysosomes can exocytose their contents partially (Figure 2c) or fully (Figure 2d). In fibroblasts, lysosomes that partially release their contents have a restricted fusion pore that allows the release of smaller (10 kDa), but not larger (500 kDa) sized dextran.²⁹ However, partially fusing astrocyte lysosomes released both small and large sized dextran (Figures 2e and g), indicating that partially exocytosing lysosomes do not have the same restricted fusion pore as in fibroblasts.²⁹ Another feature of partially exocytosing fibroblast lysosomes is that the lysosomal membrane protein (for example, CD63-GFP) does not diffuse into the plasma membrane.²⁹ Using CD63-GFP labeling we observed threefold fewer ATP-triggered exocytic events/cell (3 ± 0.9 ; Figure 2f, green circles), as compared with the luminal marker FITC dextran (10.5 ± 2.5 ; Figure 1i). This indicates that, similar to fibroblasts, partially exocytosing astrocyte lysosomes do not release CD63-GFP into the plasma membrane. When $[\text{Ca}^{2+}]_c$ in the same cell was raised further by ionomycin treatment, many of the lysosomes that had not released CD63-GFP upon ATP treatment released all of their CD63-GFP (Figure 2f, red circles), indicating ionomycin-triggered complete exocytosis. An alternate possibility is that ionomycin caused lysis of the CD63-GFP-

Figure 2 Calcium triggers partial and complete lysosome exocytosis. Images showing the cell surface LAMP1 staining of astrocytes that were (a) not injured or (b) injured by rolling glass beads in the presence of TRITC dextran, marking the injured cells red. Green labeling shows cell surface LAMP1 stained using live (unfixed) astrocytes. Scale bar indicates 10 μm . (c and d) Fate of individual lysosomes labeled with FITC dextran and monitored by TIRF imaging as the cells are injured focally by a laser – (c) a lysosome that fuses partially, releasing only a part of its luminal content; (d) a lysosome that fuses fully, releasing all of its luminal content. Scale bar indicates 1 μm . Corresponding plots show intensity traces that correspond to the circled region in the time lapse images above. (e) Time lapse images and (g) plot showing a lysosome undergoing partial fusion as it releases the small (10 kDa) and large (500 kDa) Dextran. Note that the lysosome above the circled one, which does not fuse, also does not lose any dextran fluorescence. (f) TIRFM images of an astrocyte showing CD63-GFP-labeled lysosomes before and following sequential treatment with 10 μM ATP and then 10 μM ionomycin. Green circles mark the sites where lysosomes released CD63-GFP following ATP treatment and red circle mark the sites where lysosomes released CD63-GFP following subsequent ionomycin treatment. (h) Time lapse images of a lysosome as it undergoes exocytosis leading to gradual dispersion of CD63-GFP in the plasma membrane. The plot shows the change in peak intensity of the region marked in the images by white circle and total intensity of the entire region shown in the images. Even after fusion (point of maximal peak intensity) the total fluorescence spreads in the cell membrane around the vesicle. (i–l) Relative fraction of complete and partial fusion events following Ca^{2+} increase by 10 μM . (i) ATP ($n = 7$ cells) and (j) DHPG ($n = 4$ cells), (k) ionomycin ($n = 10$ cells) and (l) injury ($n = 6$ cells). Values are mean \pm S.E.M. and assessed by Mann–Whitney U -test; * $P < 0.05$, ** $P < 0.01$ and *** $P < 0.001$

labeled lysosome. We have shown that monitoring CD63-GFP fluorescence by TIRF allows distinguishing between lysosome exocytosis and lysis.¹² As the CD63-GFP-labeled

lysosome enters the TIRF field, there is a rapid increase in vesicle-associated fluorescence intensity ('peak intensity'). Exocytosis and lysis both decrease the peak fluorescence.



Lysis causes decrease through the loss of fluorophores into the cytoplasm, whereas exocytosis causes decrease by diffusion of the fluorophores into the plasma membrane. Thus, integrated TIRF fluorescence ('total intensity') in the cell membrane plane decreases during lysis but remains constant during exocytosis.^{12,35,36} Upon ionomycin treatment, the 'total intensity' of lysosomal CD63-GFP increased and then remained constant (Figure 2f inset and corresponding plot in Figure 2h), demonstrating that CD63-GFP dispersed freely into the plasma membrane. This established that the lysosomes underwent exocytosis.

Next, we tested whether differential $[Ca^{2+}]_c$ increase affected partial or complete lysosome exocytosis. Receptor-mediated increase in $[Ca^{2+}]_c$ resulted in predominantly partial exocytosis $91 \pm 3\%$ (ATP) and $79 \pm 4\%$ (3,5-Dihydroxyphenylglycine, DHPG; Figures 2i and j), whereas injury and ionomycin caused predominantly complete exocytosis $63 \pm 1\%$ and $69 \pm 3.9\%$, respectively (Figures 2k and l). This is unlike fibroblasts, where lysosomes undergo predominantly partial exocytosis independent of the means of $[Ca^{2+}]_c$ increase.²⁹ As ionomycin and injury cause greater $[Ca^{2+}]_c$ increase as compared with ATP and DHPG, it is possible that the amplitude of $[Ca^{2+}]_c$ increase regulates the nature of (partial/complete) lysosome exocytosis. Alternately, calcium entry by ATP and DHPG may be occurring through transporters not close enough to the lysosomes to trigger full release.³⁷ This could explain the release of CD63-GFP by more lysosomes following ionomycin as compared with ATP treatment (Figure 2f). To examine the link between $[Ca^{2+}]_c$ and the nature of lysosome fusion, we next examined the involvement of synaptotagmin in this process.

Lack of Syt VII on astrocyte lysosomes facilitates Ca^{2+} -triggered exocytosis. Synaptotagmin VII is known to regulate lysosomal exocytosis;^{29,38} however, Syt VII expression in astrocytes is disputed.^{27,28} Multiple Syt VII isoforms reported in neurons and chromaffin cells.^{39,40} Mouse myoblasts expressed two Syt VII isoforms (45 and 51 kDa), whereas mouse astrocytes showed very weak expression of the 51-kDa and none of the 45-kDa isoform (Figure 3a). Whereas the 45-kDa isoform is known to localize on the vesicles, the 51-kDa isoform localizes to the cell membrane.^{39,40} To test whether the 51-kDa isoform localizes to astrocyte lysosomes, protein from the subcellular fractions of primary astrocytes were probed with anti-LAMP1 and anti-Syt VII antibodies (Figure 3b). The LAMP1-positive fractions (F1–F3) showed no Syt VII (Figure 3b) and the fraction (F6) with the 51-kDa band was devoid of lysosomes. Immunostaining showed that Syt VII was mostly diffuse, and none of the punctate Syt VII labeling colocalized with the lysosomal marker LAMP1 (Figure 3c). Thus, lysosomes in primary astrocytes do not express Syt VII. To test when expressed exogenously, can the 45-kDa isoform of Syt VII (Figure 3d) traffic to the astrocyte lysosome, a GFP-tagged 45-kDa isoform was expressed, which localized to the lysosomes (Figure 3e). This indicated that the absence of endogenous Syt VII on the astrocyte lysosomes is not due to the lack of proper trafficking machinery.

On the basis of our previous findings²⁹ that lysosomes in Syt VII knockout fibroblasts undergo complete fusion without

restricted pore size, we hypothesized that lack of Syt VII on astrocyte lysosomes may be responsible for the similar nature of lysosomal exocytosis in astrocytes (Figures 2e and h). If so, this would predict that expression of Syt VII on astrocyte lysosomes will cause reduced and predominantly partial exocytosis. Expression of Syt VII on the astrocyte lysosomes resulted in the following: (1) decreased injury-triggered lysosomal exocytosis – 13.7 ± 3.3 compared with 29.2 ± 3.3 fusion/cell/min in control transfected cells (Figure 3f); (2) increased proportion of lysosomes that underwent partial exocytosis (Figure 3g); and (3) caused a twofold increase (20 s *versus* 10 s) in the time needed for half of injury-triggered lysosome exocytosis to occur (Figure 3h). These observations establish that the lack of Syt VII on lysosomes facilitates rapid and complete exocytosis in astrocytes and suggests that another synaptotagmin isoform regulates Ca^{2+} -dependent lysosome exocytosis in astrocytes.

Syt XI regulates lysosomal exocytosis in astrocytes.

To identify the synaptotagmin that regulates lysosome exocytosis in astrocytes, we examined the synaptotagmins IV, V and XI, which are known to be expressed in astrocytes.²⁸ Whereas all these synaptotagmins showed punctate expression, only Syt XI colocalized with lysosomes (Figures 4a and b). Syt XI is the most abundant Syt isoform in astrocytes and is expressed more abundantly in the astrocytes as compared with the neurons,^{27,28,30} however, its subcellular localization in astrocytes is not known.^{41,42} Use of western blot analysis confirmed expression of Syt XI protein in primary astrocytes (Figure 4c). Using cell fractionation we found that endogenous Syt XI is enriched in the lysosome fractions (Figure 4d), demonstrating its localization on astrocyte lysosomes.

Using siRNA-mediated knockdown we tested the role of Syt XI in lysosomal exocytosis in astrocytes. Four Syt XI-specific siRNAs were pooled together or used individually; each caused >90% decrease in Syt XI expression (Figure 4e). Injury of Syt XI-depleted cells resulted in twofold increase in the number of partial lysosome exocytosis events (Figures 4f and k) and threefold decrease in the total number of lysosome exocytosis events/cell/min (Supplementary Figure 1A; Figure 4j). Depletion of Syt XI did not alter the kinetics of lysosomal exocytosis (Figure 4g), suggesting that the low level (~10%) of Syt XI in the knockdown cells may be responsible for the residual lysosomal exocytosis. To establish the specificity of Syt XI knockdown effect, we generated Syt XI cDNA with conservative base substitutions that made this cDNA (SytXI_r-GFP) refractory to one of the Syt XI siRNA – siRNA2. siRNA2 prevented expression of Syt XI-GFP, but not of SytXI_r-GFP (Figures 4h and i). SytXI_r-GFP expression not only reversed the decrease in lysosome exocytosis caused by siRNA2-mediated Syt XI knockdown, it also reversed the decrease in the fraction of complete fusion (Figures 4j and k). This established the requirement of Syt XI for Ca^{2+} -dependent exocytosis of lysosomes in astrocytes.

Lysosomal exocytosis is required for the repair of injured astrocytes. Although astrocytes can repair injury to their cell membrane,⁴³ the mechanism for this has remained enigmatic. In other cells, lysosome exocytosis facilitates

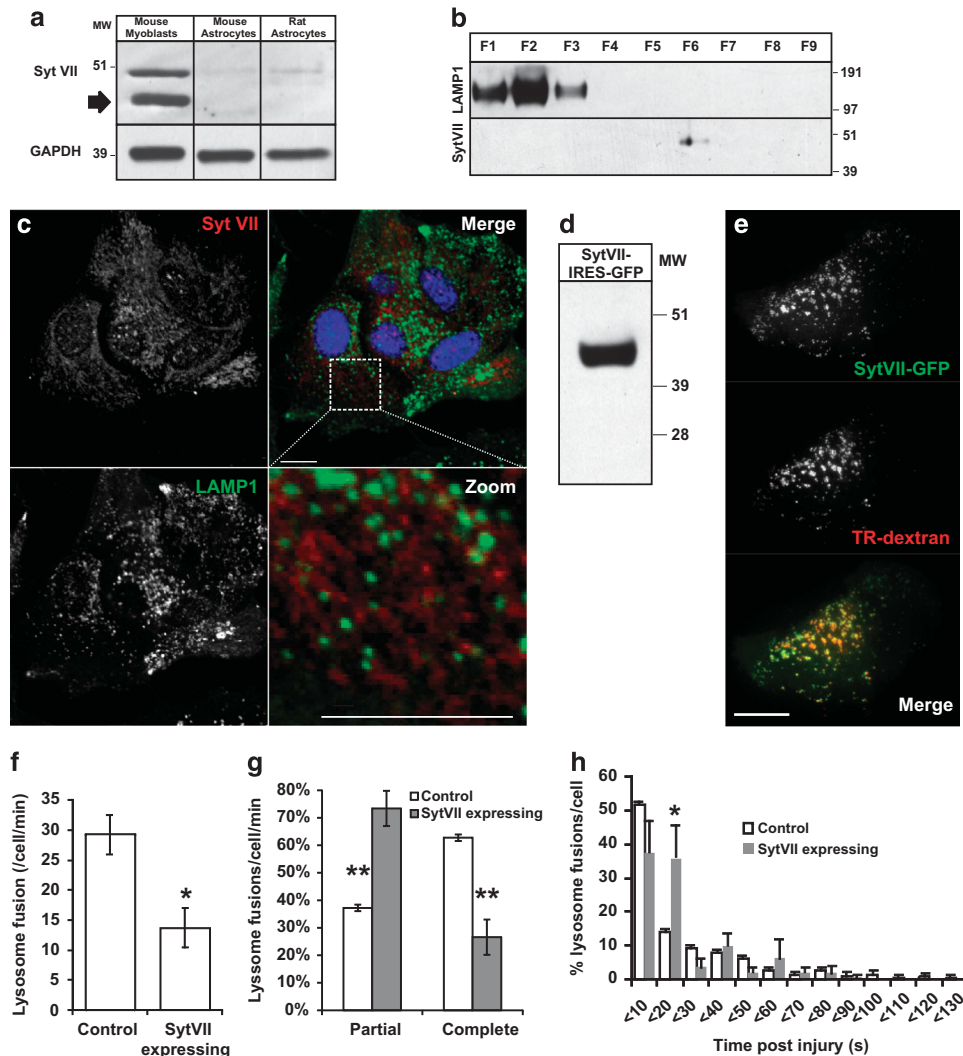


Figure 3 Synaptotagmin VII expression in astrocytes inhibits lysosomal exocytosis. (a) Western blot shows two endogenous Syt VII isoforms (50 and 45 kDa) in mouse myoblasts, one of which (the 50 kDa) is expressed at low level in rat and mouse astrocytes ($n = 6$). (b) Western blot analysis of density gradient subcellular fractions of primary astrocyte showing that the fractions enriched for the lysosomal marker LAMP1 (F1–F3) lack Syt VII immunoreactivity ($n = 3$), whereas the heavier F6 fraction lacking LAMP1 contains the 50-kDa Syt VII isoform. (c) Confocal image of astrocytes showing immunolabeling of endogenous Syt VII (top left) and LAMP1 (bottom left) show lack of colocalization (top right) and zoom of the marked region in bottom right). Scale bars indicate $10 \mu\text{m}$. (d) Representative western blot ($n = 6$) showing lysate of HEK cells transfected with IRES-GFP vector expressing 45-kDa Syt VII isoform. (e) Total internal reflection fluorescence (TIRF) images showing localization of GFP-tagged 45-kDa isoform of Syt VII (green) in a cell where the lysosomes were labeled by feeding cells with TR-dextran (red). Scale bars indicate $10 \mu\text{m}$. The merged image shows colocalization of 45-kDa Syt VII isoform with lysosomal marker LAMP1. (f) Plot showing the effect of expressing CFP-tagged 45-kDa Syt VII isoform on exocytosis of lysosomes compared with the corresponding untransfected cells on the same coverslip ($n \geq 5$ cells). Data represents mean \pm S.E.M. * $P < 0.05$ by Mann–Whitney U -test. (g) Injury-triggered partial and complete fusion of lysosomes in astrocytes not expressing (control) or expressing the CFP-tagged 45-kDa Syt VII isoform. Data represent mean \pm S.E.M. assessed by Mann–Whitney U -test; ** $P < 0.01$. (h) Kinetics of injury-triggered lysosome exocytosis in control and Syt VII-OE cells. Data represent mean \pm S.E.M. * $P < 0.05$ by two-way ANOVA followed by Bonferroni multiple comparisons. Scale bars indicate $10 \mu\text{m}$

repair of injury to their cell membrane.^{14,16} However, in view of above differences in the nature and regulation of astrocyte lysosome exocytosis, we examined whether injury-triggered lysosome exocytosis still facilitates repair of injured astrocytes. Intact cells exclude the lipophilic dyes (FM1–43, FM4–64) from the cytosol; however, injury causes these dyes to enter the cell and bind endomembrane (Supplementary Videos 2).³¹ This causes continuous increase in cellular dye fluorescence until the cell membrane is repaired and dye entry is blocked.³¹ Use of this approach established the obligate requirement of injury-triggered calcium entry for

astrocyte cell membrane repair (Figure 5a, Supplementary Figure 1B). Astrocytes injured in the presence of extracellular calcium (Figure 5a, blue curve; Supplementary Video 2), but not those injured in the absence of extracellular calcium managed to repair (Figure 5a, red curve; Supplementary Video 3). Similar to astrocytes injured in the absence of calcium, astrocytes expressing 45-kDa Syt VII isoform showed continued dye entry even 4 min after injury (Figure 5b, red curve; Supplementary Figure 1C; Supplementary Video 4). This is in contrast to astrocytes not transfected with Syt VII (control), where dye entry ceased within 30 s of injury

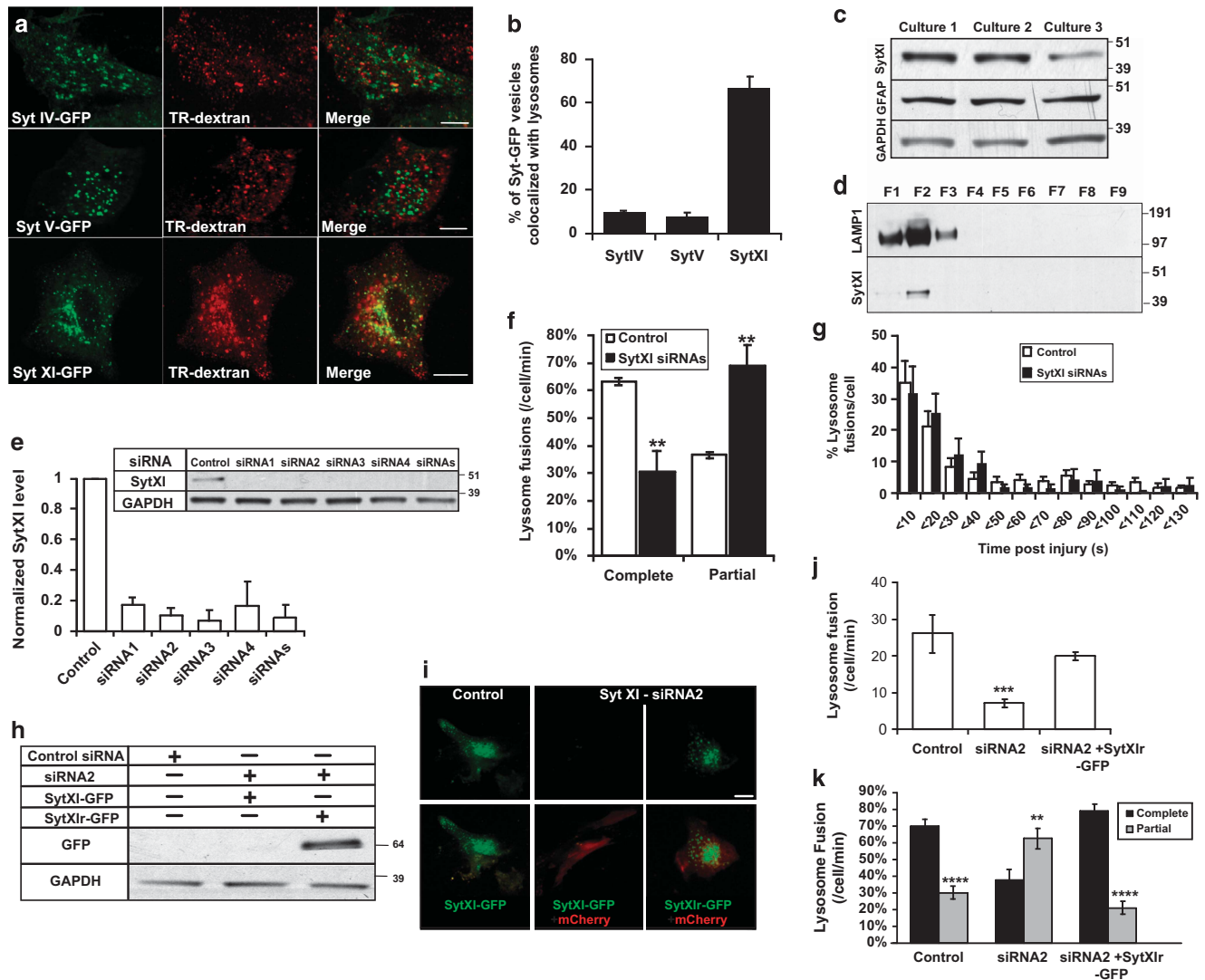
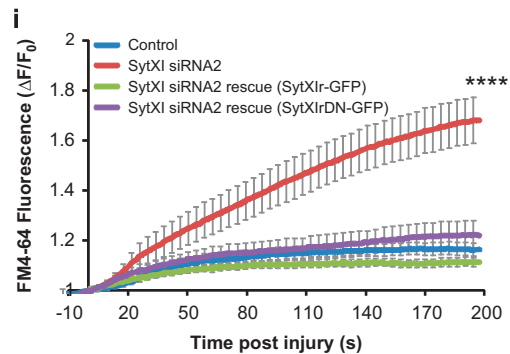
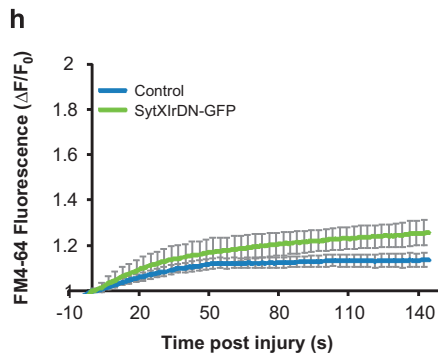
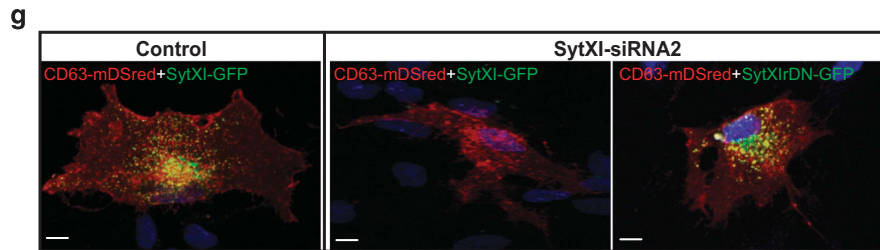
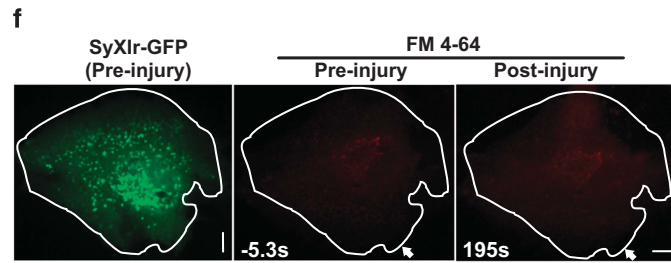
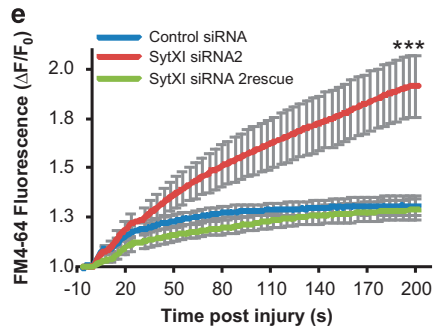
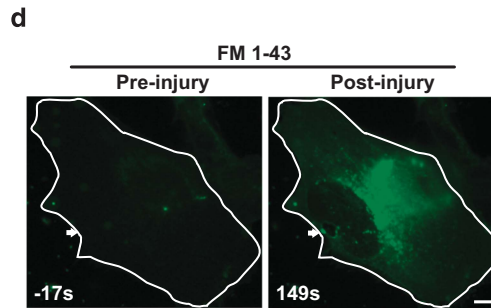
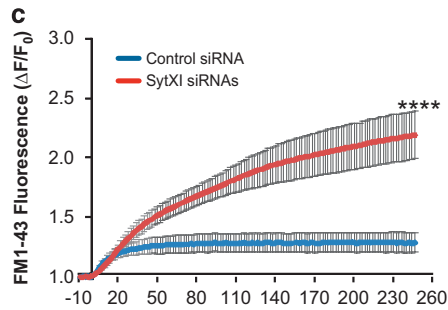
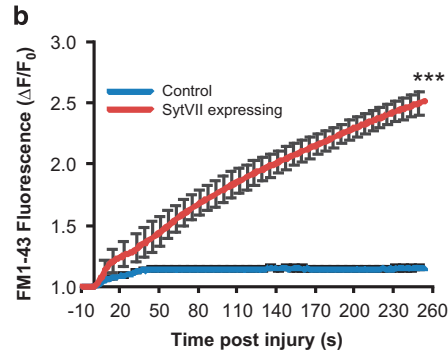
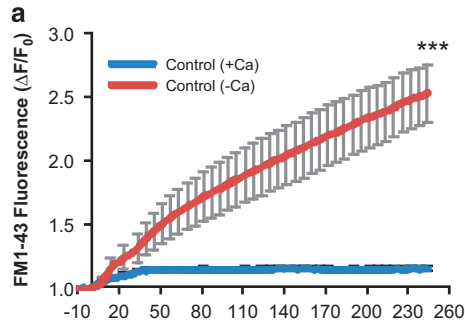


Figure 4 Synaptotagmin XI is required for Ca^{2+} -triggered lysosomal exocytosis. (a) Confocal images of mouse astrocytes showing localization of exogenously expressed Syt IV-GFP (top), Syt V-GFP (middle) and Syt XI-GFP with TR-dextran-labeled lysosomes. Scale bars indicate $10 \mu\text{m}$. (b) Quantification of colocalization of Syt IV, Syt VII and Syt XI-GFP-labeled vesicles with TR-dextran-labeled lysosomes ($n > 5$ cells). (c) A representative western blot ($n = 6$) for Syt XI in three independent mouse astrocyte cultures; GAPDH is used as loading control and GFAP is used as an astrocytic marker. (d) Representative western blot of density gradient fractions of mechanically lysed primary mouse astrocytes as described in Figure 3e and probed for LAMP1 (lysosomal marker) and Syt XI ($n = 3$). Note Syt XI is detected in the fractions (F1 and F2) most enriched for lysosomal marker LAMP1. (e) Western blot and quantification ($n = 6$) of Syt XI knockdown in astrocytes by Syt XI-specific siRNAs, individually (siRNA 1–siRNA 4) or pooled together (siRNAs). (f) Effect of Syt XI knockdown (by pooled siRNAs) on the extent of injury-triggered partial and complete fusion of lysosomes and on (g) the kinetics of injury-triggered exocytosis. (h) Representative western blot showing the effect of Syt XI-specific siRNA (siRNA2) on expression of Syt XI-GFP and SytXlr-GFP in mouse myoblasts ($n = 3$). (i) Representative epifluorescence images of mouse astrocytes transfected with control siRNA or Syt XI-siRNA2. Cells were co-transfected with mCherry (to mark transfected cells) and either Syt XI-GFP or mCherry or siRNA2-resistant SytXlr-GFP ($n > 5$ cells). Scale bars indicate $10 \mu\text{m}$. (j) Injury-triggered exocytosis of individual TRITC dextran-labeled lysosomes ($n > 4$ cells each) in astrocytes transfected with control siRNA or co-transfected with Syt XI-siRNA2 together with SytXlr-GFP ($n = 5$ cells). (k) Effect of Syt XI knockdown by Syt XI-siRNA2 and rescue by SytXlr-GFP on the extent of injury-triggered partial and complete fusion of lysosomes. Data represent mean \pm S.E.M. $**P < 0.01$, $***P < 0.001$ and $****P < 0.0001$ by Mann–Whitney U -test

Figure 5 Inhibiting lysosome exocytosis prevents the repair of injured astrocyte cell membrane. Kinetics of cell membrane repair was monitored by quantifying FM dye fluorescence intensity in astrocytes injured in presence of FM4–64 or FM1–43 dye. Plots (a–c, e, h and i) and representative images (d and f) show the FM dye labeling of astrocytes through the course of repair: (a) in the presence ($n = 6$) or absence ($n = 13$) of Ca^{2+} ; (b) with or without exogenous expression of Syt VII ($n = 6$) and (c–i) following Syt XI knockdown by (c and d) Syt XI-siRNA pool (siRNAs) or (e and f) Syt XI-siRNA2 with or without the rescue of the knockdown by using SytXlr-GFP ($n = 13$ cells each). (g) Images showing expression and colocalization of Syt XI-GFP or SytXlrDN-GFP with CD63-mDsRed in astrocytes transfected with control siRNA or Syt XI-siRNA2 ($n = 6$ cells). (h and i) Plots showing kinetics of FM4–64 dye entry in siRNA2 and SytXlrDN-GFP ($n < 22$ cells each). The sites of injury are marked in the images by the white arrow. Plot represent mean \pm S.E.M., and $***P < 0.001$, $****P < 0.0001$ by Student's t -test compared with the control. Scale bars indicate $10 \mu\text{m}$



(Figure 5b, blue curve). This provided the first evidence that inhibition of lysosome exocytosis (by Syt VII expression) inhibits cell membrane repair. However, as Syt VII is not normally expressed on astrocyte lysosomes, we next assessed astrocyte repair following inhibition of lysosome exocytosis by Syt XI knockdown. Depletion of Syt XI by a siRNA pool compromised the ability of astrocytes to repair (Figure 5c) and caused extensive cytoplasmic labeling with FM1–43 dye (Figure 5d; Supplementary Video 5). Repair was also compromised when Syt XI was depleted using siRNA2 (Figure 5e, red curve), and was fully reversed by the expression of SytXIr-GFP (Figure 5e, green curve; Figure 5f). This established that injury-triggered lysosome exocytosis, mediated by Syt XI, is required for the repair of injury to the astrocyte plasma membrane. Next, we examined whether the Syt XI regulation of lysosome exocytosis in astrocytes involves the binding of Ca^{2+} to the three aspartate residues present in the Syt XI C2B domain. SytXIr cDNA was mutated to replace Aspartates (D) with asparagines (N) to generate SytXIrDN-GFP (siRNA-resistant Syt XI cDNA with aspartate to asparagine mutation-GFP; Supplementary Figure 2). We hypothesized that if these aspartates coordinate the Ca^{2+} ion in a manner similar to Syt IV, then Syt XIrDN will inhibit Ca^{2+} -triggered lysosome exocytosis and impair the ability of the injured astrocytes to undergo repair. Using CD63 to mark late endosome/lysosome, SytXIrDN-GFP was found to efficiently localize to lysosomes (Figure 5g), and overexpression of SytXIrDN-GFP did not affect the repair capability of the astrocytes (Figure 5h). This suggested that overexpression of Syt XI lacking any Ca^{2+} -binding ability does not affect the ability of the endogenous

Syt XI to facilitate lysosome exocytosis. Next, to test the ability of Syt XIrDN-GFP to rescue the repair ability of the astrocytes lacking endogenous Syt XI, SytXIrDN-GFP was expressed in cells depleted of endogenous Syt XI (by siRNA2). SytXIrDN-GFP fully rescued the repair defect caused by the lack of endogenous Syt XI (Figure 5i). This demonstrates that Syt XI regulates astrocyte repair independent of the ability of Ca^{2+} binding to its C2 domain.

Discussion

Receptor-mediated $[\text{Ca}^{2+}]_c$ elevation in astrocytes triggers lysosome exocytosis.^{11,12,20,44} We show that astrocyte cell membrane injury causes a greater $[\text{Ca}^{2+}]_c$ increase, triggering more robust lysosome exocytosis. Receptor stimulation causes a sustained and low rate of exocytosis where lysosomes release a part of their luminal content and none of their membrane proteins (Figures 2 and 6). In contrast, cell membrane injury causes a burst of exocytic events where lysosomes release all of their luminal content and deliver their membrane proteins to the cell membrane (Figures 1,2 and 6). This response of astrocyte lysosomes to high $[\text{Ca}^{2+}]_c$ is in contrast to fibroblasts, where high $[\text{Ca}^{2+}]_c$ still triggers partial lysosome exocytosis.²⁹ Deletion of Syt VII causes rapid and complete Ca^{2+} -regulated lysosome exocytosis in fibroblast in response to high $[\text{Ca}^{2+}]_c$, indicating that Syt VII restricts the kinetics and extent of lysosomal fusion.²⁹ Lack of Syt VII on astrocyte lysosomes may be responsible for their rapid and complete exocytosis following high $[\text{Ca}^{2+}]_c$ (Figures 2 and 3). This suggestion is supported by increased partial exocytosis and decreased complete exocytosis of lysosomes when Syt

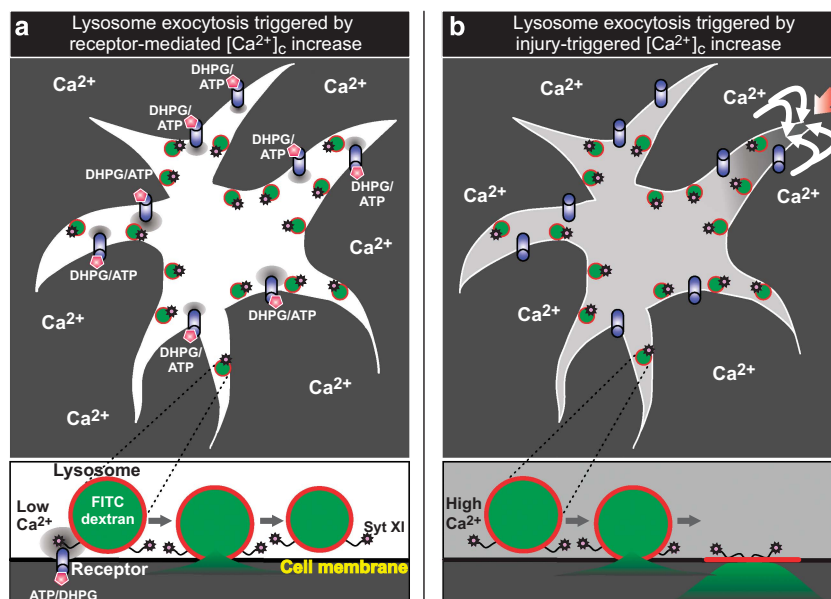


Figure 6 Schematic representation of receptor and injury-triggered lysosome exocytosis. (a) Treating astrocytes with agonists for purinergic and metabotropic receptors (blue cylinders) causes a small increase in $[\text{Ca}^{2+}]_c$ (gray puffs) through calcium influx or efflux from cell exterior or internal stores, respectively. Syt XI (but not Syt VII) facilitates the exocytosis of the lysosomes such that the fusion pore closes rapidly leading to partial release of the luminal content (green) and no mixing of the lysosomal membrane (red) with cell membrane black. (b) Astrocyte injury leading to rupture of the cell membrane (red arrow) causes large influx of extracellular calcium (gray cytosol). Here Syt XI facilitates full fusion of the lysosomes, resulting in complete release of lysosomal luminal content and mixing of the lysosomal membrane with the cell membrane, which allows for the repair of the injured cell membrane

VII is expressed on astrocyte lysosomes. We also show that astrocyte lysosomes express Syt XI, which is required for lysosomal exocytosis (Figure 4). Thus, Syt XI may also facilitate the rapid and complete lysosome exocytosis observed in WT and Syt VII lacking fibroblasts.²⁹ Our finding that Syt XI localizes to lysosomes and is required for exocytosis of lysosomal membrane protein is in agreement with Syt XI localization to endosome/lysosome in macrophages and its deficit causing reduced delivery of lysosomal membrane proteins to the macrophage cell membrane.⁴⁵

Unlike synaptotagmins such as Syt VII, the C2A domains of Syt XI and Syt IV lack calcium and calcium-dependent phospholipid-binding ability *in vitro*.^{46,47} Despite the lack of Ca²⁺ binding by the Syt IV and Syt XI C2A domains,⁴⁶ Syt IV facilitates regulated exocytosis in neurons, astrocytes and endocrine cells.^{28,48–50} Similarly, Syt XI-containing vesicles undergo depolarization-triggered exocytosis in neurons.⁴² Similar to neuronal lysosomes,⁵¹ Syt XI-containing exocytic vesicles in neurons are acidic in nature and localize to dendrites.⁴² To test whether, similar to Syt IV, the C2B domain of Syt XI helps trigger exocytosis, we mutated the three putative Ca²⁺-binding aspartate (D) residues in the C2B domain of Syt XI to asparagines (N) (SytXIrdN). This mutant protein rescued the knockdown of endogenous Syt XI as efficiently as WT Syt XI, indicating that Syt XI-regulated lysosome exocytosis does not require Ca²⁺ binding to C2 domains. A Ca²⁺-independent role attributed to synaptotagmin was illustrated by SytI mutant, which lacks Ca²⁺ binding in both its C2 domains and facilitates vesicle docking.⁵² Ca²⁺-independent role of SytI is also supported by its ability to facilitate close membrane apposition *in vitro* even in the absence of calcium binding^{24–26} and the recent identification of Ca²⁺-independent SNARE-binding motifs.⁵³ Syt XI may similarly facilitate lysosome docking to the cell membrane. Such a mode of action of Syt XI would recapitulate our recent finding with an unrelated C2 domain containing protein called dysferlin, which facilitated injury-triggered lysosome exocytosis by tethering lysosomes to the cell membrane.³¹ As it is the cell membrane proximal lysosome that undergo Ca²⁺-triggered exocytosis,³⁴ docking lysosome to the cell membrane may be a critical regulatory step for Ca²⁺-triggered lysosomal exocytosis, defect in which compromises cell membrane repair. Another mechanism by which Syt XI may regulate lysosome exocytosis is through interaction with the Q-SNARE Vti1a.⁵⁴ Vti1a is known to interact with the lysosomal R-SNARE VAMP7 and regulate spontaneous neurotransmission as well as stimulated secretion.^{55,56}

Lysosomal exocytosis facilitates ATP secretion by astrocytes and mechanical injury triggers ATP release from astrocytes.^{20,57} ATP released by astrocytes activates AKT and ERK signaling, resulting in gliosis following traumatic brain injury.^{58,59} Injury-triggered extracellular ATP also affects microglial response following brain injury.^{60,61} We have identified that injury-triggered lysosome exocytosis causes secretion of acid sphingomyelinase (ASM), which is needed for cell membrane repair.¹⁶ ASM secretion by glial cells is also triggered by ATP, which in turn regulates secretion of inflammatory cytokines.⁵⁷ Thus, by releasing ASM and ATP in response to injury, lysosome exocytosis can coordinate repair of brain injury at both the cellular and tissue levels. Syt

XI could thus be a regulator of the roles attributed to astrocytes in regulation of repair following acute brain injury.⁹ Such a role of Syt XI may explain its involvement in neurodegenerative disorders including schizophrenia and Parkinson's.^{62–65} Thus, our findings provide cellular and molecular mechanism for repair of injured astrocytes, and suggest a potential mechanism for the involvement of Syt XI in brain injury repair.

Materials and Methods

Cell culture and transfection. All experiments involving animals were conducted under the Institutional Animal Care and Use Committee (IACUC guidelines). Animals were maintained in a facility accredited by the American Association for Accreditation of Laboratory Animal Care. For primary astrocytes we used a method based on Hertz.⁶⁶ Briefly, brain from P0 to P1 pup of C57/Bl6 mouse was removed by decapitation and was immediately put in ice-cold HBSS (without Ca and Mg). Optical bulb, hind brain and meninges were removed under a stereomicroscope (Zeiss stemi 2000, Carl Zeiss Microscopy, LLC, Thornwood, NY, USA) and both the cortical hemispheres minced and digested for 30 min at 37 °C in 0.25% Trypsin (GIBCO, Bridgewater, NJ, USA). After 10 triturations, the sample was transferred to pre-warmed Astrocyte Growth Medium (AGM) and cells were collected by centrifugation 1000xg for 5 min. The cell pellet was resuspended in pre-warmed AGM and passed through a 70- μ m syringe filter to remove lumps. The cell suspension was grown on a 25-cm² flask for 5–7 days at 37 °C and 5% CO₂ concentration. When the cells were confluent, the flask was shaken overnight at 37 °C and 230 r.p.m. (Incushaker Mini, Benchmark, Edison, NJ, USA). Microglia and oligodendrocytes floating in the media were discarded, and the adherent astrocytes were collected with 1 \times Trypsin for further use. Astrocytes and HEK293T cells were cultured in DMEM with L-Glutamine and high glucose (PAA, Pasching, Austria), supplemented with fetal bovine serum FBS (PAA; 20% for AGM, 10% for regular media) and with Penicillin/Streptomycin (P/S; PAA). Cells were treated with 10 μ M ATP (for purinergic signaling), with 10 μ M DHPG (for metabotropic glutamate signaling), or with 10 μ M calcium ionophore – ionomycin (for direct calcium increase).

Plasmid transfection and siRNA knockdown. Astrocytes were transfected with plasmids using Lipofectamine 2000 (Life Technologies, Carlsbad, CA, USA) as per the manufacturer's instructions and were allowed express for 48 h. HEK293T cells were transfected with plasmids using Eugene HD (Promega, Madison, WI, USA), and harvested after 48 h. The Syt XI siRNAs used in this study include the following: siRNA 1 (5'-GCACAGUCUGAGCGAGUAC-3'), siRNA2 (5'-AUGUCAAGGUGAACGUCUA-3'), siRNA3 (5'-GAGAGAGGUCUGCGAGAGU-3') and siRNA4 (5'-CGAUCGCACUACUAGAAGU-3') and were transfected using Lipofectamine RNAiMAX (Life Technologies)

Immunoblot and immunostaining. Cells grown to 70–80% confluence were lysed with RIPA buffer (Sigma-Aldrich, St. Louis, MO, USA) containing protease inhibitor cocktail (Fisher Scientific, Waltham, MA, USA). Proteins resolved on a 4–12% gradient gel (Life Technologies) were transferred to a nitrocellulose membrane and probed using the following antibodies: Syt VII (1 : 300), Syt XI (1 : 1000; Synaptic Systems, Göttingen, Germany), lysosome-associated membrane protein 1 (LAMP1; 1 : 200; Santa Cruz, Dallas, TX, USA), GAPDH (1 : 1000; Santa Cruz) overnight at 4 °C. This was followed by binding for an hour with HRP-conjugated appropriate secondary antibody (Sigma-Aldrich) For immunostaining, cells were fixed with chilled methanol and after blocking for 1 h with PBS containing 5% Normal Goat Serum (NGS, Sigma) were probed overnight at 4 °C with above primary antibodies: Syt VII (1 : 200), LAMP1 (1 : 300) in blocking solution. Fluorophore-conjugated secondary antibodies (1 : 500) in 5% NGS were incubated for 1 h at room temperature, and nuclei were stained with Hoechst 33342. After mounting in Immunogold mounting medium (Life Technologies) cells were imaged with motorized Olympus FV1000 confocal microscope (\times 40/1.30 NA oil or \times 60/1.40 NA oil or \times 100/1.40 NA oil objectives) controlled using the FV10ASW3.0 software (Olympus America, Center Valley, PA, USA).

Lysosome isolation. The cells (packed volume 0.3 ml; 300 million cells) were disrupted in a Dounce homogenizer and the lysate was centrifuged at 1000xg for 10 min and supernatant was centrifuged at 20 000xg for 20 min. The pellet was layered on top of an OptiPrep (Sigma) gradient and centrifuged for 4 h at 4 °C

150 000 × g in MLA55 rotor in Beckman Coulter (Indianapolis, IN, USA) Optima Max-XP Ultracentrifuge. Fractions (~600 μl each; F1–F9) were collected from top to bottom with a fine tipped pipette, protein-estimated and processed for immunoblot. Presence of lysosome was validated with an anti-LAMP1 antibody.

Live imaging of lysosomal exocytosis. Cells were subjected to live imaging of cell membrane for injury-triggered lysosome assay as described.³¹ Untransfected or astrocytes transfected with Syt VII-CFP were incubated overnight with growth media containing 2 mg/ml of FITC dextran. The cells were washed and incubated for 2 h with growth medium. Cells were then transferred to the microscope stage top ZILCS incubator (Tokai Hit Co, Shizuoka-ken, Japan) maintained at 37 °C. For laser injury, cells were imaged with TIRF at the penetration depth of 70–120 nm by imaging at four to six frames/s for 3 min using IX81 Olympus microscope (Olympus America) equipped with ×60/1.45 NA oil objective and 488 nm and Evolve 512 EMCCD (Photometrics, Tucson, AZ, USA) camera, diode laser of 488 nm (Cobolt, Solna, Sweden). Acquisition and analysis was carried out using Slidebook 5.0 and 5.5 (Intelligent Imaging Innovations Inc., Denver, CO, USA).

Cell membrane injury assays. The glass bead injury assay was performed as demonstrated previously.³¹ The assay was performed as shown before.³¹ Untransfected or Syt VII-transfected, Syt XI knocked down astrocytes cultured on coverslips were transferred to Attofluor cell chamber (Life Technologies), incubated in cell imaging media (CIM) with calcium/PBS buffer with 1 μg/μl FM1–43 dye or 2.5 μg/μl FM4–64 (Life Technologies) and placed on a Tokai Hit microscopy stage top ZILCS incubator (Tokai Hit Co) maintained at 37 °C. For laser injury, a 1–2-μm²-area was irradiated for <100 ms with a pulsed laser (Ablate!, 3i Intelligent Imaging Innovations Inc. Denver, CO, USA). Cells were imaged at 1–10 s intervals for 5 min using IX81 Olympus microscope (Olympus America) equipped with Lambda DG-4 (Sutter Instruments, Novato, CA, USA) widefield illumination system and Evolve 512 EMCCD (Photometrics) camera, with Cell-TIRFM (Olympus) illuminator and ×60/1.45 NA oil objective using Slidebook 5.0 and 5.5 (Intelligent Imaging Innovations Inc.). Results were expressed as ratio of FM dye intensity over intensity before injury.

Measurement of intracellular calcium. Astrocytes were cultured on glass coverslips and incubated in DMEM with 10 μM of Fluo-4-AM (Life Technologies) for 20 min at 37 °C and 5% CO₂. After washing with pre-warmed cell imaging media (CIM),³¹ cells were laser-injured as described previously³¹ and imaged at four to eight frames/s. Change in cytosolic Ca²⁺ was measured as the ratio change in fluorescence over the background subtracted Fluo-4 fluorescence ($\Delta F/F_0$, F_0 is Fluo-4 intensity before treatment and ΔF indicates the increase in fluorescence over F_0).

Quantification and statistical analysis. The fluorescence intensity of images was quantified using Slidebook 5.0 and 5.5 (Intelligent Imaging Innovations Inc.) or Metamorph7.0 (Molecular Devices, Sunnyvale, CA, USA). The statistical analysis was carried out using the GraphPad Prism Software (GraphPad, LaJolla, CA, USA).

Conflict of Interest

The authors declare no conflict of interest.

Acknowledgements. We thank Cotrina Marisa, Xiaoqin Fu and Judy Liu for technical help, Mitsunori Fukuda for providing GFP-tagged synaptotagmins, and Kristy Brown for editing the manuscript. SCS and JKJ carried out the work and wrote the manuscript. TT, MN and SMS contributed new reagents, analytical approaches and helped write the manuscript. This work was supported by the National Institutes of Health Grants R01AR055686 (NIAMS), P50AR060836 (NIAMS) and P30HD040677 (NICHD) to JKJ.

- Nedergaard M. Direct signaling from astrocytes to neurons in cultures of mammalian brain cells. *Science* 1994; **263**: 1768–1771.
- Parpura V, Zorec R. Gliotransmission: exocytotic release from astrocytes. *Brain Res Rev* 2010; **63**: 83–92.
- Pasti L, Zonta M, Pozzan T, Vicini S, Carmignoto G. Cytosolic calcium oscillations in astrocytes may regulate exocytotic release of glutamate. *J Neurosci* 2001; **21**: 477–484.

- Bezzi P, Carmignoto G, Pasti L, Vesce S, Rossi D, Rizzini BL et al. Prostaglandins stimulate calcium-dependent glutamate release in astrocytes. *Nature (London)* 1998; **391**: 281–285.
- Calegari F, Coco S, Taverna E, Bassetti M, Verderio C, Corradi N et al. A regulated secretory pathway in cultured hippocampal astrocytes. *J Biol Chem* 1999; **274**: 22539–22547.
- Coco S, Calegari F, Pravettoni E, Pozzi D, Taverna E, Rosa P et al. Storage and release of ATP from astrocytes in culture. *J Biol Chem* 2003; **278**: 1354–1362.
- Pangrsic T, Potokar M, Stenovc M, Kreft M, Fabbretti E, Nistri A et al. Exocytotic release of ATP from cultured astrocytes. *J Biol Chem* 2007; **282**: 28749–28758.
- Christopherson KS, Ullian EM, Stokes CC, Mullen CE, Hell JW, Agah A et al. Thrombospondins are astrocyte-secreted proteins that promote CNS synaptogenesis. *Cell* 2005; **120**: 421–433.
- Chen Y, Swanson RA. Astrocytes and brain injury. *J Cereb Blood Flow Metab* 2003; **23**: 137–149.
- Hamilton NB, Attwell D. Do astrocytes really exocytose neurotransmitters? *Nat Rev Neurosci* 2010; **11**: 227–238.
- Li D, Ropert N, Koulakoff A, Giaume C, Oheim M. Lysosomes are the major vesicular compartment undergoing Ca²⁺-regulated exocytosis from cortical astrocytes. *J Neurosci* 2008; **28**: 7648–7658.
- Jaiswal JK, Fix M, Takano T, Nedergaard M, Simon SM. Resolving vesicle fusion from lysis to monitor calcium-triggered lysosomal exocytosis in astrocytes. *Proc Natl Acad Sci USA* 2007; **104**: 14151–14156.
- Han WQ, Xia M, Xu M, Boini KM, Ritter JK, Li NJ et al. Lysosome fusion to the cell membrane is mediated by the dysferlin C2A domain in coronary arterial endothelial cells. *J Cell Sci* 2012; **125**: 1225–1234.
- Reddy A, Caler EV, Andrews NW. Plasma membrane repair is mediated by Ca(2+)-regulated exocytosis of lysosomes. *Cell* 2001; **106**: 157–169.
- Chakrabarti S, Kobayashi KS, Flavell RA, Marks CB, Miyake K, Liston DR et al. Impaired membrane resealing and autoimmune myositis in synaptotagmin VII-deficient mice. *J Cell Biol* 2003; **162**: 543–549.
- Defour A, Van der Meulen JH, Bhat R, Bigot A, Bashir R, Nagaraju K et al. Dysferlin regulates cell membrane repair by facilitating injury-triggered acid sphingomyelinase secretion. *Cell Death Dis* 2014; **5**: e1306.
- Stinchcombe J, Bossi G, Griffiths GM. Linking albinism and immunity: the secrets of secretory lysosomes. *Science* 2004; **305**: 55–59.
- Andrews NW. Regulated secretion of conventional lysosomes. *Trends Cell Biol* 2000; **10**: 316–321.
- Sivaramakrishnan V, Bidula S, Campwala H, Katikaneni D, Fountain SJ. Constitutive lysosome exocytosis releases ATP and engages P2Y receptors in human monocytes. *J Cell Sci* 2012; **125**: 4567–4575.
- Zhang Z, Chen G, Zhou W, Song A, Xu T, Luo Q et al. Regulated ATP release from astrocytes through lysosome exocytosis. *Nat Cell Biol* 2007; **9**: 945–953.
- Verderio C, Cagnoli C, Bergami M, Francolini M, Schenk U, Colombo A et al. TI-VAMP/VAMP7 is the SNARE of secretory lysosomes contributing to ATP secretion from astrocytes. *Biol Cell* 2012; **104**: 213–228.
- Sudhof TC. A molecular machine for neurotransmitter release: synaptotagmin and beyond. *Nat Med* 2013; **19**: 1227–1231.
- Sudhof TC, Rizo J. Synaptotagmins: C2-domain proteins that regulate membrane traffic. *Neuron* 1996; **17**: 379–388.
- Kim JY, Choi BK, Choi MG, Kim SA, Lai Y, Shin YK et al. Solution single-vesicle assay reveals PIP2-mediated sequential actions of synaptotagmin-1 on SNAREs. *EMBO J* 2012; **31**: 2144–2155.
- Lin CC, Seikowski J, Perez-Lara A, Jahn R, Hobartner C, Walla PJ. Control of membrane gaps by synaptotagmin-Ca²⁺ measured with a novel membrane distance ruler. *Nat Commun* 2014; **5**: 5859.
- Wang Z, Liu H, Gu Y, Chapman ER. Reconstituted synaptotagmin I mediates vesicle docking, priming, and fusion. *J Cell Biol* 2011; **195**: 1159–1170.
- Mittelstaedt T, Seifert G, Alvarez-Baron E, Steinhilber C, Becker AJ, Schoch S. Differential mRNA expression patterns of the synaptotagmin gene family in the rodent brain. *J Comp Neurol* 2009; **512**: 514–528.
- Zhang Q, Fukuda M, Van Bockstaele E, Pascual O, Haydon PG. Synaptotagmin IV regulates glial glutamate release. *Proc Natl Acad Sci USA* 2004; **101**: 9441–9446.
- Jaiswal JK, Chakrabarti S, Andrews NW, Simon SM. Synaptotagmin VII restricts fusion pore expansion during lysosomal exocytosis. *PLoS Biol* 2004; **2**: E233.
- Zhang Y, Chen K, Sloan SA, Bennett ML, Scholze AR, O'Keefe S et al. An RNA-sequencing transcriptome and splicing database of glia, neurons, and vascular cells of the cerebral cortex. *J Neurosci* 2014; **34**: 11929–11947.
- Defour A, Sreetama SC, Jaiswal JK. Imaging cell membrane injury and subcellular processes involved in repair. *J Vis Exp* 2014; **85**: e51106.
- Holroyd P, Lang T, Wenzel D, De Camilli P, Jahn R. Imaging direct, dynamin-dependent recapture of fusing secretory granules on plasma membrane lawns from PC12 cells. *Proc Natl Acad Sci USA* 2002; **99**: 16806–16811.
- Gandhi SP, Stevens CF. Three modes of synaptic vesicular recycling revealed by single-vesicle imaging. *Nature (London)* 2003; **423**: 607–613.

34. Jaiswal JK, Andrews NW, Simon SM. Membrane proximal lysosomes are the major vesicles responsible for calcium-dependent exocytosis in nonsecretory cells. *J Cell Biol* 2002; **159**: 625–635.
35. Jaiswal JK, Simon SM. Imaging single events at the cell membrane. *Nat Chem Biol* 2007; **3**: 92–98.
36. Schmoranzler J, Goulian M, Axelrod D, Simon SM. Imaging constitutive exocytosis with total internal reflection fluorescence microscopy. *J Cell Biol* 2000; **149**: 23–32.
37. Simon SM, Llinás RR. Compartmentalization of the submembrane calcium activity during calcium influx and its significance in transmitter release. *Biophys J* 1985; **48**: 485–498.
38. Martínez I, Chakrabarti S, Hellevik T, Morehead J, Fowler K, Andrews NW. Synaptotagmin VII regulates Ca(2+)-dependent exocytosis of lysosomes in fibroblasts. *J Cell Biol* 2000; **148**: 1141–1150.
39. Sugita S, Han W, Butz S, Liu X, Fernandez-Chacon R, Lao Y *et al*. Synaptotagmin VII as a plasma membrane Ca(2+) sensor in exocytosis. *Neuron* 2001; **30**: 459–473.
40. Fukuda M, Ogata Y, Saegusa C, Kanno E, Mikoshiba K. Alternative splicing isoforms of synaptotagmin VII in the mouse, rat and human. *Biochem J* 2002; **365**: 173–180.
41. Yeo H, Kim HW, Mo J, Lee D, Han S, Hong S *et al*. Developmental expression and subcellular distribution of synaptotagmin 11 in rat hippocampus. *Neuroscience* 2012; **225**: 35–43.
42. Dean C, Dunning FM, Liu H, Bomba-Warczak E, Martens H, Bharat V *et al*. Axonal and dendritic synaptotagmin isoforms revealed by a pHluorin-syt functional screen. *Mol Biol Cell* 2012; **23**: 1715–1727.
43. Ellis EF, McKinney JS, Willoughby KA, Liang S, Povlishock JT. A new model for rapid stretch-induced injury of cells in culture: characterization of the model using astrocytes. *J Neurotrauma* 1995; **12**: 325–339.
44. Liu T, Sun L, Xiong Y, Shang S, Guo N, Teng S *et al*. Calcium triggers exocytosis from two types of organelles in a single astrocyte. *J Neurosci* 2011; **31**: 10593–10601.
45. Arango DG, Fukuda M, Descoteaux A. Synaptotagmin XI regulates phagocytosis and cytokine secretion in macrophages. *J Immunol* 2013; **190**: 1737–1745.
46. Dai H, Shin OH, Machius M, Tomchick DR, Südhof TC, Rizo J. Structural basis for the evolutionary inactivation of Ca2+ binding to synaptotagmin 4. *Nat Struct Mol Biol* 2004; **11**: 844–849.
47. von Poser C, Ichtchenko K, Shao X, Rizo J, Südhof TC. The evolutionary pressure to inactivate. A subclass of synaptotagmins with an amino acid substitution that abolishes Ca2+ binding. *J Biol Chem* 1997; **272**: 14314–14319.
48. Johnson SL, Franz C, Kuhn S, Furness DN, Rüttiger L, Munkner S *et al*. Synaptotagmin IV determines the linear Ca2+ dependence of vesicle fusion at auditory ribbon synapses. *Nat Neurosci* 2010; **13**: 45–52.
49. Robinson IM, Ranjan R, Schwarz TL. Synaptotagmins I and IV promote transmitter release independently of Ca(2+) binding in the C(2)A domain. *Nature (London)* 2002; **418**: 336–340.
50. Mori Y, Higuchi M, Hirabayashi Y, Fukuda M, Gotoh Y. JNK phosphorylates synaptotagmin-4 and enhances Ca2+-evoked release. *EMBO J* 2008; **27**: 76–87.
51. Schwenk BM, Lang CM, Hogl S, Tahirovic S, Orozco D, Rentzsch K *et al*. The FTLD risk factor TMEM106B and MAP6 control dendritic trafficking of lysosomes. *EMBO J* 2014; **33**: 450–467.
52. Lee J, Guan Z, Akbergenova Y, Littleton JT. Genetic analysis of synaptotagmin C2 domain specificity in regulating spontaneous and evoked neurotransmitter release. *J Neurosci* 2013; **33**: 187–200.
53. Zhou Q, Lai Y, Bacaj T, Zhao M, Lyubimov AY, Uervirojngkoorn M *et al*. Architecture of the synaptotagmin-SNARE machinery for neuronal exocytosis. *Nature (London)* 2015; **525**: 62–67.
54. Milochau A, Lagree V, Benassy MN, Chaignepain S, Papin J, Garcia-Arcos I *et al*. Synaptotagmin 11 interacts with components of the RNA-induced silencing complex RISC in clonal pancreatic beta-cells. *FEBS Lett* 2014; **588**: 2217–2222.
55. Ramirez DM, Khvotchev M, Trauterman B, Kavalali ET. Vti1a identifies a vesicle pool that preferentially recycles at rest and maintains spontaneous neurotransmission. *Neuron* 2012; **73**: 121–134.
56. Bose A, Guilherme A, Huang S, Hubbard AC, Lane CR, Soriano NA *et al*. The v-SNARE Vti1a regulates insulin-stimulated glucose transport and Acrp30 secretion in 3T3-L1 adipocytes. *J Biol Chem* 2005; **280**: 36946–36951.
57. Bianco F, Perrotta C, Novellino L, Francolini M, Riganti L, Menna E *et al*. Acid sphingomyelinase activity triggers microparticle release from glial cells. *EMBO J* 2009; **28**: 1043–1054.
58. Neary JT, Kang Y, Willoughby KA, Ellis EF. Activation of extracellular signal-regulated kinase by stretch-induced injury in astrocytes involves extracellular ATP and P2 purinergic receptors. *J Neurosci* 2003; **23**: 2348–2356.
59. Franke H, Sauer C, Rudolph C, Krugel U, Hengstler JG, Illes P. P2 receptor-mediated stimulation of the PI3-K/Akt-pathway *in vivo*. *Glia* 2009; **57**: 1031–1045.
60. Davalos D, Grutzendler J, Yang G, Kim JV, Zuo Y, Jung S *et al*. ATP mediates rapid microglial response to local brain injury *in vivo*. *Nat Neurosci* 2005; **8**: 752–758.
61. Orr AG, Orr AL, Li XJ, Gross RE, Traynelis SF. Adenosine A(2A) receptor mediates microglial process retraction. *Nat Neurosci* 2009; **12**: 872–878.
62. Brzustowicz LM, Hodgkinson KA, Chow EW, Honer WG, Bassett AS. Location of a major susceptibility locus for familial schizophrenia on chromosome 1q21-q22. *Science* 2000; **288**: 678–682.
63. Yokota H, Tsujita T, Okazaki Y, Kikuya E, Oishi M. Polymorphic 33-bp repeats with promoter-like activity in synaptotagmin 11 gene. *DNA Res* 2003; **10**: 287–289.
64. Inoue S, Imamura A, Okazaki Y, Yokota H, Arai M, Hayashi N *et al*. Synaptotagmin XI as a candidate gene for susceptibility to schizophrenia. *Am J Med Genet B Neuropsychiatr. Genet* 2007; **144B**: 332–340.
65. Huynh DP, Scoles DR, Nguyen D, Pulst SM. The autosomal recessive juvenile Parkinson disease gene product, parkin, interacts with and ubiquitinates synaptotagmin XI. *Hum Mol Genet* 2003; **12**: 2587–2597.
66. Hertz L, Lovatt D, Goldman SA, Nedergaard M. Adrenoceptors in brain: cellular gene expression and effects on astrocytic metabolism and [Ca(2+)]_i. *Neurochem Int* 2010; **57**: 411–420.

Supplementary Information accompanies this paper on Cell Death and Differentiation website (<http://www.nature.com/cdd>)